

ISSNe 1678-4596 RURAL ENGINEERING



VIS-NIR-SWIR spectroscopy in sugarcane (Saccharum officinarum L.) cultivation for phytosanitary purposes

Natália Correr Ré^{1*} Carlos Augusto Alves Cardoso Silva¹
Ana Karla da Silva Oliveira¹ Matheus Luís Caron¹
Matheus Sterzo Nilsson¹ Daniel Garbellini Duft¹ Peterson Ricardo Fiorio¹

ABSTRACT: One of the causes of productivity loss in sugarcane cultivation has been associated with the species *Diatraea saccharalis*, also known as the sugarcane borer. Therefore, this study evaluated the feasibility of using hyperspectral sensors to obtain the leaf spectral response of sugarcane in different periods of infestation at leaf and canopy levels to diagnose *D. saccharalis* damage in advance. The study included three varieties of sugarcane: CTC9003BT, CTC4, and RB966928. The insecticide Altacor® was used to control pestsin half of the plots. Data collection occurred at the following stages: sprouting, tillering, stalke longation, and early maturation. Data regarding relative water content (RWC), leaf spectral signature in the laboratory and canopy, vegetation indices (NDVI and MCARI), productivity, purity, and total recoverable sugar (TRS) were collected to evaluate the borer effects on the sugarcane crop. The highest RWC was observed for CTC9003BT (60.15%) without insecticide and 59.0% with insecticide. The visible (400-680 nm) and near-infrared (750-1300 nm) spectral bands identified spectral variations in plants with and without sugarcane borer. The percentage of sugarcane borer showed high and negative correlations between productivity, NDVI, and TRS, with coefficients of -0.68, -0.76, and -0.76, respectively. The NDVI and MCARI indices effectively detect plants under stress, but their variation is influenced by multiple factors, making it difficult to associate them with a single problem (sugarcane borer). Key words: sensing, spectroscopy, *Diatraea saccharalis*.

Espectroscopia VIS-NIR-SWIR na cultura da cana-de-açúcar (Saccharum officinarum L.) para fins fitossanitários

RESUMO: Uma das causas de perda de produtividade em lavouras de cana está associada à espécie Diatraea saccharalis, também conhecida por broca da cana. Portanto, este estudo avaliou a viabilidade do uso de sensores hiperespectrais para obter a resposta espectral foliar da canade-açúcar em diferentes períodos de infestações, tanto a nível foliar quanto dossel, a fim de diagnosticar antecipadamente os danos da Diatraea saccharalis. O estudo contou com três variedades de cana-de-açúcar: CTC9003BT, CTC4 e RB966928. Em metade das parcelas foi utilizado o inseticida Altacor® para o controle de pragas. As coletas de dados ocorreram nas fases: brotação, perfilhamento, crescimento de colmos e início da maturação. Para avaliar os efeitos da broca na cana foi coletado os dados referentes ao conteúdo relativo de água (CRA), assinatura espectral foliar em laboratório e dossel, índices de vegetação (NDVI e MCARI), produtividade, pureza e ATR (Açúcar Total Recuperável). O maior CRA encontrado foi para a CTC9003BT (60,15%) sem inseticida e 59,0% com inseticida. As faixas espectrais do visível (400-680 nm) e infravermelho próximo (750-1300 nm) identificaram variações espectrais nas plantas com e sem broca. O percentual de broca apresentou correlações altas e negativas entre a produtividade, NDVI e ATR, com coeficientes de -0,68, -0,76 e -0,76, respectivamente. Os índices NDVI e MCARI foram eficazes na detecção de plantas sob estresse, contudo, sua variação é influenciada por múltiplos fatores, sendo dificil associá-los a um único problema (broca).

Palavras-chave: sensoriamento, espectroscopia, Diatraea saccharalis.

INTRODUCTION

The sugarcane production chain has been gaining ground in Brazilian agribusiness along with increased demand for renewable energy (MEDINA & POKORNY, 2022). In a more current scenario, global sugarcane cultivation in 2017 was recorded with a production of 1841 million tons (Mt), with Brazil holding the position of main producer, with almost 41% of this production, followed by India and China (SILALERTRUKSA & GHEEWALA, 2020). Thus, sugar cane is considered one of the great alternatives

for the biofuels sector (TURDERA, 2013). This topic has greater importance and engagement, especially as concern about global warming and dependence on fossil fuels grows (CANABARRO et al., 2023).

Concurrent with the expansion of areas with sugarcane cultivars, problems related to pest attacks can cause losses to the sector. One of the main pests responsible for part of this economic loss is the species *Diatraea saccharalis*, also known as sugarcane borer (FOGLIATA et al., 2022; OLIVEIRA et al., 2022). The borer *D. saccharalis* is an insect that presents holometabolic development, that is,

Departamento de Engenharia de Biossistemas, Escola Superior de Agricultura "Luiz de Queiroz", Universidade de São Paulo (USP), 13418-900, Piracicaba, SP, Brasil. E-mail: natalia.re@alumni.usp.br. *Corresponding author.

it undergoes complete metamorphosis during its development, as it goes through the stages of egg (4 to 9 days), larva (40 to 60 days), pupa (9 to 14 days), and adult (5 to 7 days), with the total cycle reaching 59 to 90 days (CARBOGNIN et al., 2023). The attack by this species occurs during the larval phase, which results in a reduction in stalk weight, a decrease in sucrose content, an increase in tillers, stalk breakage by the wind, and aerial rooting (CARBOGNIN, 2019; CTC, 2017). Overall, losses caused by the sugarcane borer reach 5 billion reais per year due to the reduction in agricultural and industrial productivity and sugar quality and insecticide costs (CTC, 2017).

Investments in genetic improvement have grown in recent years, mainly with the dissemination of Bt (Bacillus thuringiensis) technology, aiming to maximize sugarcane productivity and guarantee food security. This technology aims to reduce production costs, preserve biodiversity in treated areas, and obtain resistance to insect pests in agricultural systems. The Bt gene has already been used in the Center-South region of Brazilto contain D. saccharalis. In addition to the Bt gene, the sugarcane borer control involves strategies for monitoring and predicting the occurrence of target stages (CTC, 2021). However, there are difficulties in sampling newly hatched eggs and larvae, in addition to adversities in field monitoring (CARBOGNIN, 2019). In this case, hyperspectral VIS-NIR-SWIR sensing represents a strategy that can help identify D. saccharalis infestations in sugarcane fields through changes in leaf spectral reflectance. This technique has shown potential when used to assess damage caused by Bemisia tabaci (Gennadius) on soybean (BARROS et al., 2021), Nilaparvata lugens (brown planthopper) on rice (LIU & SUN, 2016; PRASANNAKUMAR et al., 2014), and Aphis gossypii (aphid) on cotton (CHEN et al., 2018). Most of these studies could identify variations in the leaf spectra of plants that were infected.

The study of the spectral behavior of targets is conducted in laboratory and field experiments, and the radiometric quantity used to express this behavior is given by a measurement capable of estimating their reflectance. In the case of vegetation, the average curve of photosynthetically active vegetation is separated into three spectral regions: visible–VIS (350-720 nm), near-infrared-NIR (720-1300 nm), and shortwave infrared-SWIR (1300-2500 nm), depending on the factors that condition their behavior (MORAES NOVO, 2010). In this sense, the use of VIS-NIR-SWIR hyperspectral data in the search for more detailed answers beyond the simple categorization of

infestation versus non-infestation has been promising (BARROS et al., 2021). It occurs because the capture of electromagnetic energy reflected by vegetation at the leaf or canopy level helps identify changes in the physiological behavior of the plant, chemical composition, and physical properties of plant tissues (BAUER, 1985), consequently analyzing the vegetation vigor (FIORIO et al., 2024).

In this context, would it be possible to use a hyperspectral sensor in sugarcane cultivation to assess the discriminatory capacity of the spectral response between healthy varieties and those infected by *D. saccharalis*? Based on this question, this research analyzed the spectral response of the sugarcane varieties CTC9003BT (genetically modified), CTC4, and RB966928 in different periods of *D. saccharalis* infestations in the leaves and canopy to diagnose borer damage to sugarcanein advance.

MATERIALS AND METHODS

Location and characterization of the study area

This study was conducted with the support of the Sugarcane Technology Center (CTC) in one of its experimental areas on the Santa Maria farm, located in the municipality of Cesário Lange-SP, Brazil, between the geographic coordinates 23°11′20″ south latitude and 47°51'34" west longitude. The local climate is Cwa, according to the Köppen climate classification (ALVARES et al., 2013; ASSUMPÇÃO et al., 2020). The experiment was set up in November 2021 with plots differentiated by varieties. Each plot consisted of six rows 12 m long and 6 m wide. The insecticide Altacor® was also used in half of the plots to control pests. This study was conducted in the 2021/2022 growing season, with the first harvest of the trial in October 2022. Three varieties of sugarcane were included in the study: CTC9003BT (genetically modified), CTC4, and RB966928. Data collections were chosen to cover the following sugarcane developmental stages: sprouting (December 2021), tillering (January 2022), stalk elongation (March 2022), and early maturation (April 2022), as shown in figure 1.

According to the Technical Leaflet, CTC9003BT is recommended for planting in type A, B, and C production environments and is usually harvested between April and September. Resistance to *D. saccharalis*, adaptability to mechanized harvesting, rare flowering, high values of tons of sugarcane per hectare (TSH) and total recoverable sugar (TRS), and long industrial processing period (IPP) stand out for this variety. The CTC4 variety

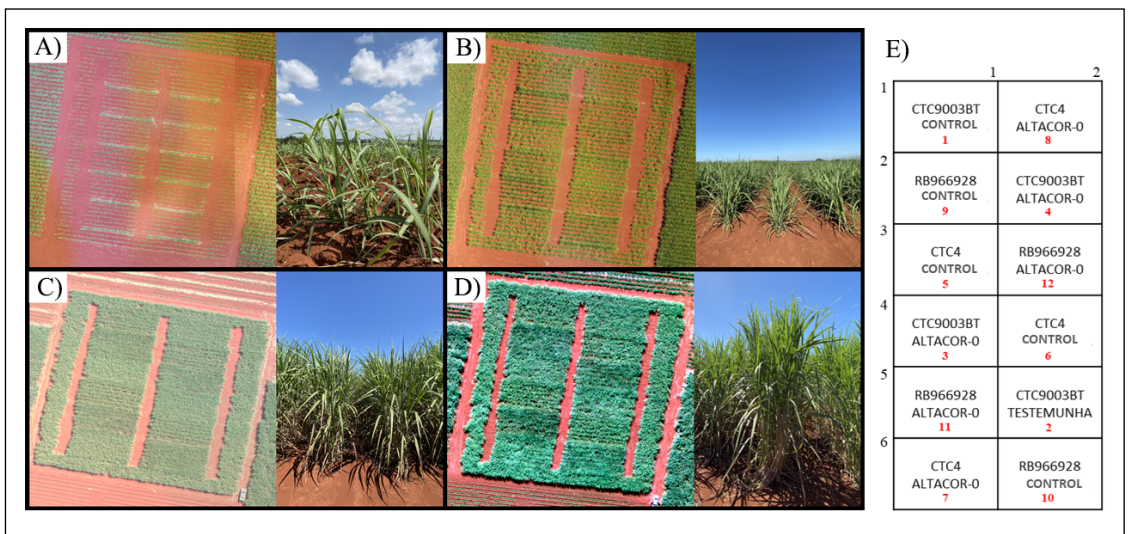


Figure 1 - Experimental area at the following stages: A) sprouting/December 2021, B) tillering/January 2022, C) stalk elongation/March 2022, and D) early maturation/April 2022; E) sketch of the trial (plot number in red).

is recommended for type A, B, C, and D production environments, standing out high TSH, adaptability to mechanized harvesting, and high tillering. Greater tolerance to sugarcane rust in plant cane is achieved by avoiding planting in January and February, while it is suggested not to extend the harvest from September for ratoon cane (CTC, 2021). The RB966928 variety presents excellent germination in plant cane, very good sprouting in ratoon cane, high tillering with excellent inter-row closure, high agricultural production, medium IPP, and early to medium maturity (RIDESA, 2010).

Acquisition of hyperspectral data (leaf and canopy)

The spectral curves were obtained using 20 leaves collected per plot for each variety. This procedure was repeated at the sprouting, tillering, stalk elongation, and early maturation stages. For collection standardization purposes, the leaves chosen for analysis were the "+1" described in the literature as a diagnostic leaf for sugarcane, which is the first leaf with the separation point between the leaf blade and the sheath (FIORIO et al., 2024). After collection, the leaves were packed in plastic bags with their respective identification and placed in a thermal box with ice to maintain their turgidity until they were taken to the laboratory of geoprocessing. The journey from the experimental area to the laboratory lasted, on average, one hour.

The spectral reading of the leaves was obtained in the laboratory using the Fieldspec® spectroradiometer (ASD-Analytical Spectral Devices

Inc., Boulder, CO, USA), which measures reflectance between 350 and 2500 nm, with a spectral resolution of 1nmfrom 350 to 1000 nm and 2 nm from 1000 to 2500 nm, with a 25° field of view. The spectrometer was turned on for 30 minutes before readings to warm up and stabilize the halogen lamp present in the equipment. Furthermore, calibration was performed with the Lambertian plate present in the sensor's leaf clip. The calibration procedure was repeated every five readings to ensure data uniformity.

After reading all 240 leaves, the spectral data were exported to the software ViewSpec Pro (ASD - Analytical Spectral Devices Inc., Boulder, CO, USA), responsible for converting them into reflectance. Furthermore, the data were pre-processed in Microsoft Excel® and the wavelengths from 350 to 449 nm and 2450 to 2500 were removed aiming to suppress noise. Therefore, the final curve covered the lengths from 450 to 2450 nm.

A Hand Held 2 spectroradiometer (ASD - Analytical Spectral Devices, Boulder, USA), which is a portable passive hyperspectral sensor that works with wavelengths from the visible to near-infrared spectrum (325 to 1075 nm), with a 3-nmspectral resolution, was used in the field at the end of the experiment and only in the fourth collection (April 2022) for sensing the plant canopy. The instrument was attached to a ruler to reach the vegetation canopy. The sensor was calibrated after every five readings with the white barium sulfate (BaSO₄) plate, which corresponds to 100% reflectance.

Similar to the data obtained from Fieldspec®, all 240 readings were exported to the software ViewSpec Pro (ASD - Analytical Spectral Devices Inc., Boulder, CO, USA) and converted into reflectance. The data was pre-processed in Microsoft Excel® and wavelengths from 325 to 399 nm and post-800nm were removed to reduce noise. Therefore, the final curve included lengths from 400 to 800 nm.

Determination of relative water content (RWC)

Water availability is a determining factor in plant productivity (LASSALLE, 2021) and relative water content (RWC) can be one of the parameters used to estimate the amount of water in a leaf (STRABELI et al., 2023). Therefore, all leaves were cut before weighing the samples using a 25-mm diameter circular scrapbook hole punch to standardize the process. The fresh weight of leaf samples (FW in grams) was measured to determine RWC. Subsequently, the leaves were stored in a plastic bag containing distilled water for 24 hours and their turgid weight (TW in grams) was measured the end of the process. Finally, the last step consisted of drying all the samples inside a previously perforated paper bag at a temperature of 70 °C in an oven for 72 hours and weighing them again to obtain the dry weight (DW in grams).

$$RWC = \frac{FW - DW}{TW + DW} \times 100 \tag{1}$$

where RWC is the relative water content (%), FWis the leaf fresh weight (g), TW is the turgid weight (g), and DW is the dry weight (g).

Red-edge normalized difference vegetation index - $NDVI_{(705)}$

The red-edge normalized difference vegetation index (NDVI ₇₀₅), calculated as a linear combination of spectral reflectance at 750 and 705 nm, is designed for hyperspectral data. NDVI utilizes the bands along the red edge and is sensitive to changes in chlorophyll content and leaf structure. Furthermore, NDVI detects subtle variations in bio-optical responses caused by the diseased canopy (KUNDU et al., 2021). The most common applications include precision agriculture, forest monitoring, forest fires, and plant stress detection (CUNDILL et al., 2015). The NDVI was determined by Equation (2). The index value varies from –1 to 1. This step was only applied to canopy hyperspectral data referring to the fourth collection.

NDVI (705) =
$$\frac{R(750) - R(705)}{R(750) + R(705)}$$
 (2)

in which R(750) and R(705) represent the spectral

reflectance in the bands of 750 nm (near infrared) and 705 nm (red edge), respectively.

Modified chlorophyll absorption ratio index (MCARI)

The modified chlorophyll absorption ratio index (MCARI) (DAUGHTRY, 2000) quantifies small canopy-scale changes in chlorophyll for different stress levels and damage sites (Equation 3) (MULLA, 2013; ZHAO et al., 2023). Low MCARI values are attributed to high leaf chlorophyll concentration (WU et al., 2008). This step was only applied to canopy hyperspectral data from the fourth collection.

MCARI(670,700) =

$$(R700 + R670) - 0.2 * (R700 - R550)$$

$$\frac{R700}{R670} \tag{3}$$

where R(700), R(670), and R(550) represent the spectral reflectance in the bands of 700 nm (near infrared), 670 nm (red), and 550 nm (green), respectively.

Assessment of Diatraea saccharalis infestation and harvest

The final assessment of *D. saccharalis* infestation was performed by the CTC team. The sugarcane borer infestation intensity was estimated by collecting and evaluating 100 stalks (or more) per plot to measure the number of borer internodes and total internodes (GALLO et al., 2002). Infestation intensity (II) =

100 * (number of borer internodes)

The occurrence of infestation was recognized visually throughout the four collections, and, in these cases, a blue ribbon was tied to the stalk to facilitate identification. The mechanized harvest was performed on October 19, 2022, and TSH and TRS data were obtained.

Pearson's correlation (r) and principal component analysis (PCA)

Pearson's correlation was calculated between the variables of productivity, purity, TRS, vegetation indices (NDVI and MCARI), and percentage of infestation. The coefficient r is a statistical measure of linear correlation between two quantitative variables, which ranges from -1 to 1. The closer to 1, the correlation is positive, and the variables increase together linearly; when close to -1, the correlation is negative. While one variable increases, the other decreases, and a coefficient equal to or close to 0 (zero) indicates no correlation.

Qualitative analyses are conducted to detect nuances across the electromagnetic spectrum. It covers aspects such as variations in reflectance intensities (albedo) and detection of absorption patterns. Principal component analysis is among the most common ones for hyperspectral data (BARROS et al., 2021; SILVA et al., 2023). PCA is a linear orthogonal transformation, which modifies the original dataset into a compressed dataset of uncorrelated variables, known as principal components (PCs) (SILVA JUNIOR; PACHECO, 2021). Therefore, PCA is a technique used to reduce the dimensionality of datasets and increase interpretability without losing information. Analyses using boxplot and Pearson's correlation were conducted using the software RStudio.

RESULTS AND DISCUSSION

Principal component analysis (PCA)

Principal components (PCs) 1, 2, and 3 represented at least 97% of the reflectance variance of the hyperspectral data. PC1 presented values of 73.10%, 71.00%, 74.40%, 84.00%, and 85.80%, PC2 of 16.34%, 19.50%, 17.10%, 9.60%, and 12.20%, and PC3 of 7.90%, 7.10%, 6.40%, 4.30%, and 0.76% for the first (leaf), second (leaf), third (leaf), fourth (leaf), and fourth (canopy) collection, respectively (Figure 2).

Similarly, RIBEIRO (2022) worked with the varieties IACSP 01-3127 and IACSP 95-5094, used components 1 and 2 (98.57% and 0.72% of the observed variance, respectively), and separated the varieties, but the materials overlapped each other. SILVA et al. (2023) worked with nutritional K stress in sugarcane and found in the principal component analysis that PC1 and PC2 explained 97% of the reflectance variance. TAVARES (2017) studied reflectance spectroscopy in response to nitrogen fertilization in sugarcane and obtained at least 99% variation in PCA with just PC1 and PC2. FRANCESCHINI et al. (2013) obtained a result of 75.8% of the spectral variability in PC1 for the evaluation of soil texture by reflectance spectroscopy, and part of the radiometric data was strongly related to clay and sand contents.

Figure 3 (A, B, C, and D) shows the scatterplots of the scores and the behavior of loadings in components 1, 2, and 3 obtained from the spectral curves for the four collections of hyperspectral data from the leaves. Considering the phenological stage of the first collection (sprouting and emergence) and that the leaf area was still very narrow, the loadings in PC1 showed influence across the entire spectrum, with peaks close to 1400 nm in the first maximum of absorption by water in the mid-infrared. PC2 also showed peaks close to the mid-infrared and close to the water absorption bands in the mid-infrared (1950 and 2450 nm). For CP3, the most influential loadings occurred in the visible region (450-700 nm), with peaks close to 670 and 680 nm, the beginning of the red-edge region, as well as participation in the three absorption maxima by water (1400, 1950, and 2450 nm) (Figure 3A).

In the second collection (Figure 3B), PC1 behaved similarly to the previous one, as the loadings

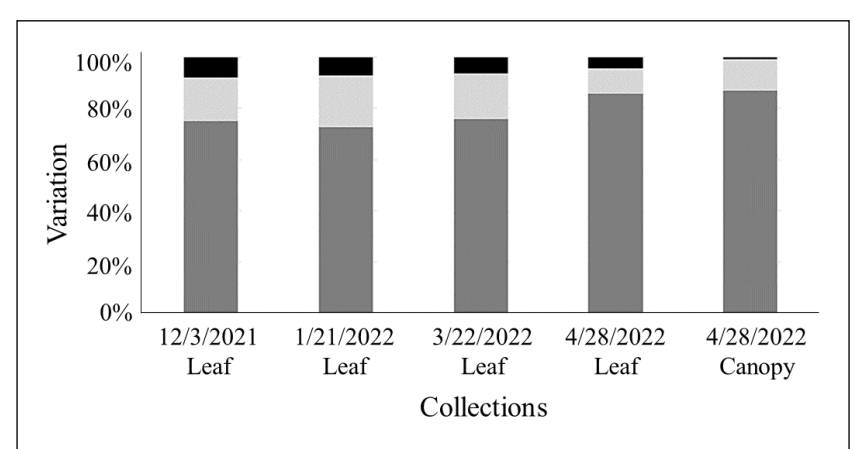


Figure 2 - Percentages of principal components (PC) 1, 2, and 3, in the collections conducted on 12/3/2021 (leaf), 1/21/2022 (leaf), 3/22/2022 (leaf), 4/28/2022 (leaf), and 4/28/2022 (canopy).

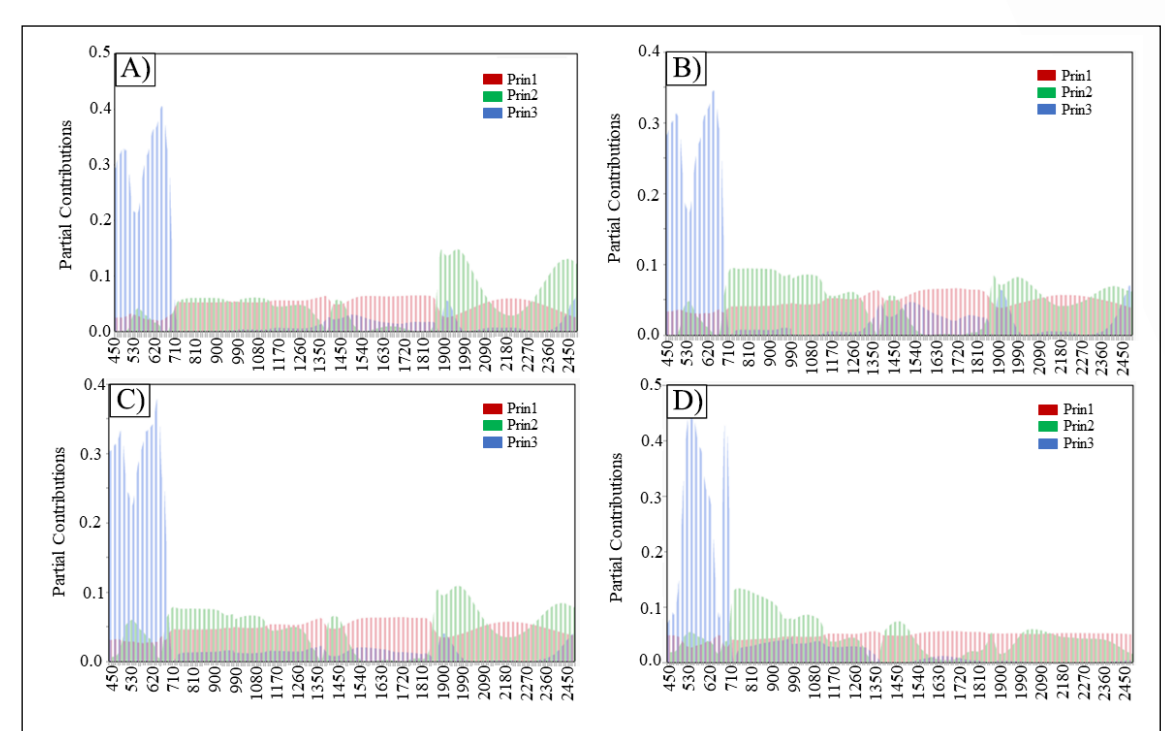


Figure 3 - Behavior of loadings in the A) first, B) second, C) third, and D) fourth collections. Prin 1, 2, and 3 represent the loadings for the principal components PC1, PC2, and PC3, respectively, indicating the contribution of each original variable to the respective component.

also showed predominance throughout the spectrum, with ends close to 1400 nm and around 1700 nm, and at 1450 and 1950 (in the water absorption bands) practically throughout the mid-infrared, with the least influential bands being observed in the visible (450-700 nm). PC2 showed maximum values close to 900 nm in the near-infrared and around 2000 nm in the mid-infrared. The behavior in PC3 was the same as that identified in the first collection, but with a little more influence on the three maxima of absorption by water (1400, 1950, and 2450 nm) and influential loadings in the visible region (450-700 nm), with peaks near 670 and 680, the beginning of the red-edge region.

The third collection showed once again the PC1 trend across the entire spectrum. PC2 manifested a little more, albeit minimally, in the visible region, with peaks around 900 nm in the near-infrared and 1400 nm in one of the water absorption bands. However, it reappeared close to 2000 nm in the midinfrared. The PC3 trend was practically identical to the second collection in the visible region (450-700 nm), with peaks in loadings close to 670 and 680, the beginning of the red-edge region, but with a low influence on the first water absorption band at 1400 nm (Figure 3C).

Finally, the PC1 loadings for the fourth collection - leaf (Figure 3D) showed an even more regular influence across the entire spectrum when compared to the other collections. This time, PC2 had peaks in the red-edge region (750 nm), located between the visible and near-infrared regions, in addition to a certain influence on the first water absorption band at 1400 nm. Furthermore, PC3 presented valleys at 450 nm and 670, while there was a jump in the red edge, specifically at 710 nm, and a higher influence in the near-infrared compared to the other collections.

The behavior of the loadings in the canopy data (Figure 4) was studied separately, as the wavelength at which the sensor works is shorter, and the range analyzed was from 400 to 900 nm. As observed, the loadings of PC1 and PC2 had a regular influence on the entire spectrum, corresponding to 98% of the spectral variability. A certain peak of PC1 was observed around 730 nm in the red-edge range as PC2 presented a valley in this same near-infrared region. Furthermore, the highest influence for PC3, equivalent to only 0.76% variation, was in the visible region (with peaks at 400nm) and around 670 nm (near infrared).

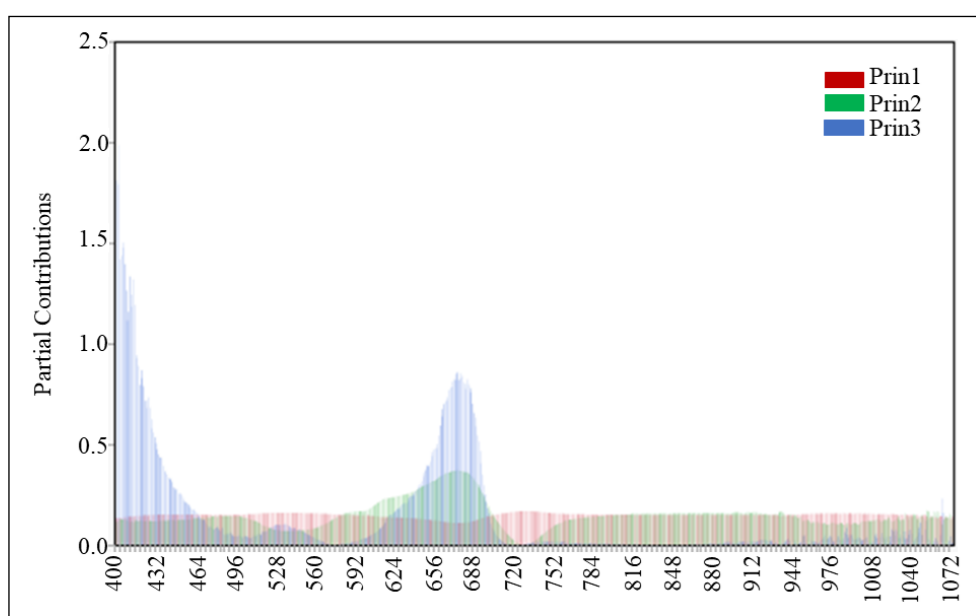


Figure 4 - Behavior of loadings in the fourth collection (canopy). Prin 1, 2, and 3 represent the loadings for the principal components PC1, PC2, and PC3, respectively, indicating the contribution of each original variable to the respective component.

Descriptive analysis of spectral curves

Figure 5 (A, B, C, and D) shows the leaf spectral behavior of the four collections. The reflectance values in the visible region (400 to 700 nm) for the first collection (December 3, 2021) (Figure 5A) did not differ much and were more subtle, whereas the range of 700 to 1300 nm (near infrared) showed the highest discrepancy between plots. However, the leaves in this first collection were still narrow and the central vein made readings difficult, which may have influenced the lack of uniformity of the data, as the plants were at the sprouting/emergence stage under the same water conditions and without the presence of the sugarcane borer in the crop.

The reflectance values in the visible region (400 to 700 nm) in the second collection (January 1, 2022) (Figure 5B) were more disparate when compared to the first collection. Plots 1 and 2 (both CTC9003BT) were those that reflected least in the visible region, signs of healthier leaves, as the amount of radiation reflected by plants is inversely related to the radiation absorbed by plant pigments and varies with the wavelength of the incident radiation (MULLA, 2013). Plant pigments, such as chlorophyll, strongly absorb radiation in the visible spectrum from 400 to 700 nm (PINTER et al., 2003). Moreover, plot 2 recorded a lower reflectance factor at the wavelength of 1950 nm, that is, as water absorbs electromagnetic radiation, plants with higher water

content in the leaf show a lower reflectance factor at this length (STRABELI et al., 2020, 2023).

For the third collection (March 22, 2022) (Figure 5C), plots 1 and 2 (CTC9003BT) absorbed more than the other plots in the visible region. Conversely, plot 6 (CTC4) reflected the most in the same region. The near-infrared range (700 to 1300 nm), a region influenced by the internal leaf structure (SINCLAIR et al., 1971), showed changes in the reflectance intensity between plots. For plots 4 and 11, the decrease in absorption of electromagnetic energy at 970 and 1200 nm is noticeable, being associated with leaf water content (ZHANG et al., 2010). Plots 3 and 9 showed the highest absorbance in the mid-infrared, specifically in the region where the maximum absorption by water is found (1400 and 1950 nm), indicating a higher water concentration in the leaf. It occurred because a strong increase of reflectance around 1450 and 1950 nm symbolizes a modification in the water status of stressed plants (JONG et al., 2012).

The plots in the fourth and final collection of leaves (Figure 5D) behaved similarly in the visible region (400 to 700 nm) compared to the other collections. In the near-infrared region, plots 1 and 2 (CTC9003BT), 3 and 4 (CTC9003BT Altacor), and 6 (CTC4) presented reflectance rates close to 50%. As for the mid-infrared, the leaves were collected in the morning at around 9:00 am, while the canopy reading was conducted on the same day at noon to

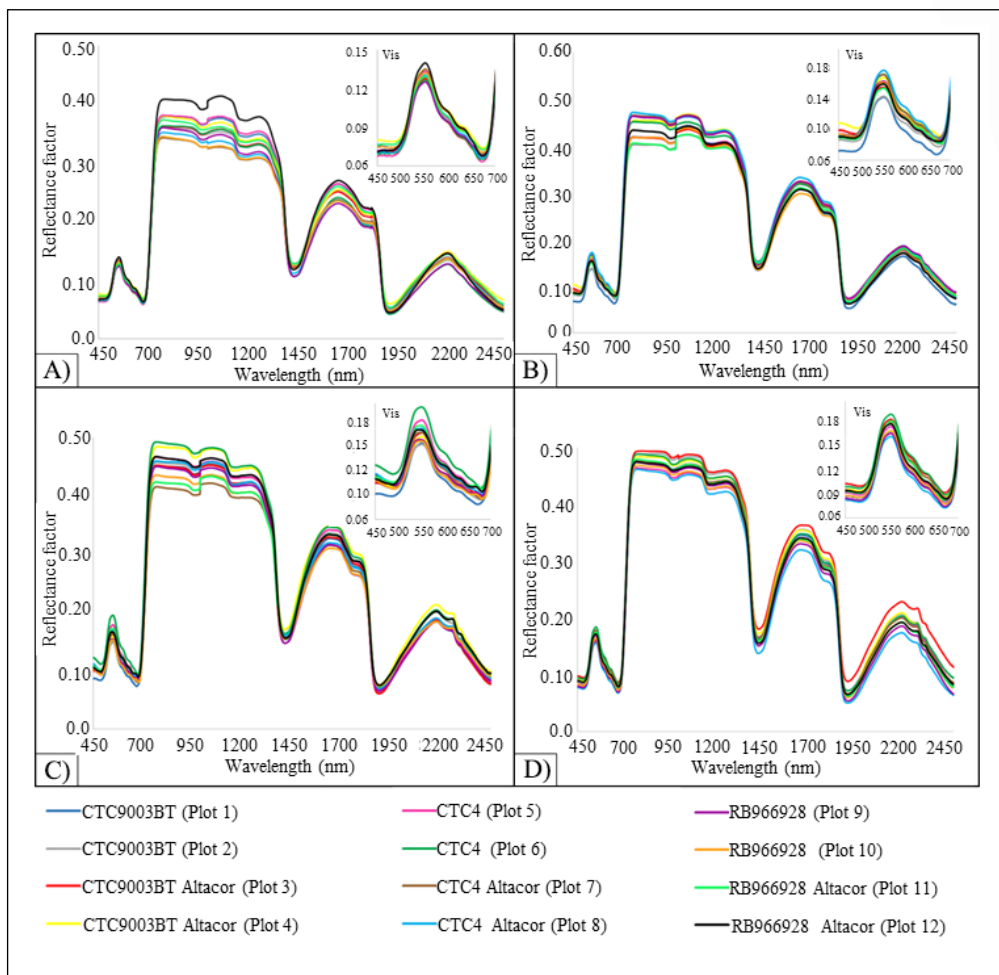


Figure 5 - Fieldspec spectroradiometer signatures (leaf): A) first collection (12/3/2021), B) second collection (1/21/2022), C) third collection (3/22/22), and D) fourth collection (4/28/2022).

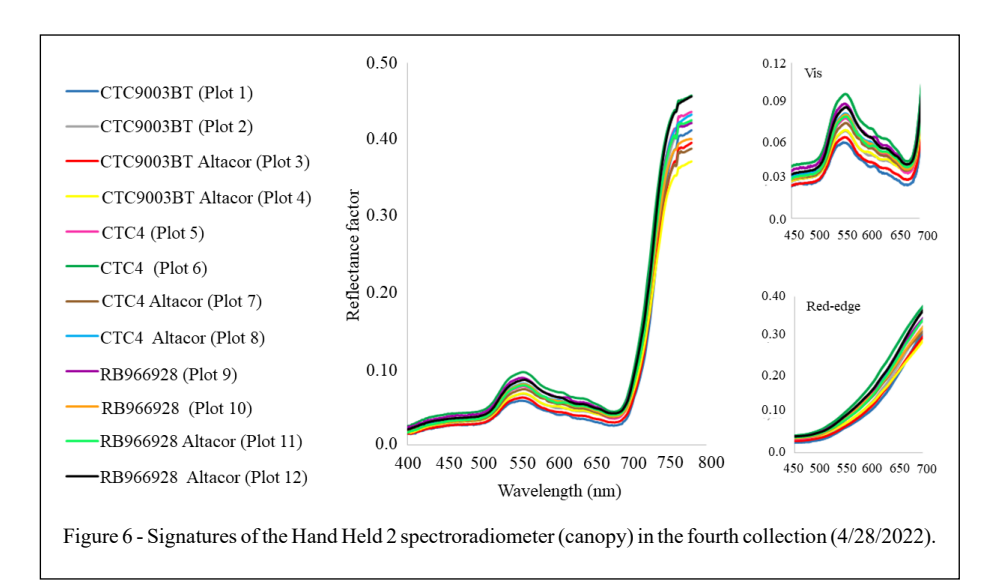
reduce the incidence of shadow on the sensor. Under these conditions, the leaves spent a long time in the thermal box and were probably unable to maintain full moisture until arrival at the laboratory.

Canopy data (Figure 6) in the red-edge range (680-750 nm), a transition region of rapid change in leaf reflectance caused by the strong absorption of pigments in the red spectrum and leaf scattering in the near-infrared, described as sensitive to chlorophyll in the crop canopy (CLEVERS et al., 2002; HATFIELD et al., 2008), showed that plots 1 and 2 (CTC9003BT) and 3 and 4 (CTC9003BT Altacor) moved most towards on the right, that is, they possibly have higher concentrations of chlorophyll and, consequently, higher energy absorption and less stress. The absence of chlorophyll leads to a decrease in energy in the visible spectral region, with higher reflectance in green and red, giving it a yellowish or chlorotic appearance

(CARTER, 1991; CHO & SKIDMORE, 2006), and the curve tends to shift to the left.

Similarly, MARTINS & GALO (2015) spectrally characterized healthy sugarcane and those infected by nematodes and *Migdolus fryanus*. Spectroradiometric measurements were conducted in situ and the analysis of spectral curves allowed the evaluation of the potential for determining the red edge position determination (REPD) and different indices such as NDVI and MCARI (derived from hyperspectral data), sensitive to chlorophyll variation in discriminating between healthy and infected crops.

ABDEL-RAHMAN et al. (2010) studied two popular sugarcane varieties grown in South Africa (N19 and N12) at different damage levels of thesugarcane thrips *Fulmekiola serrata* (Kobus). The spectral readings revealed significant differences in

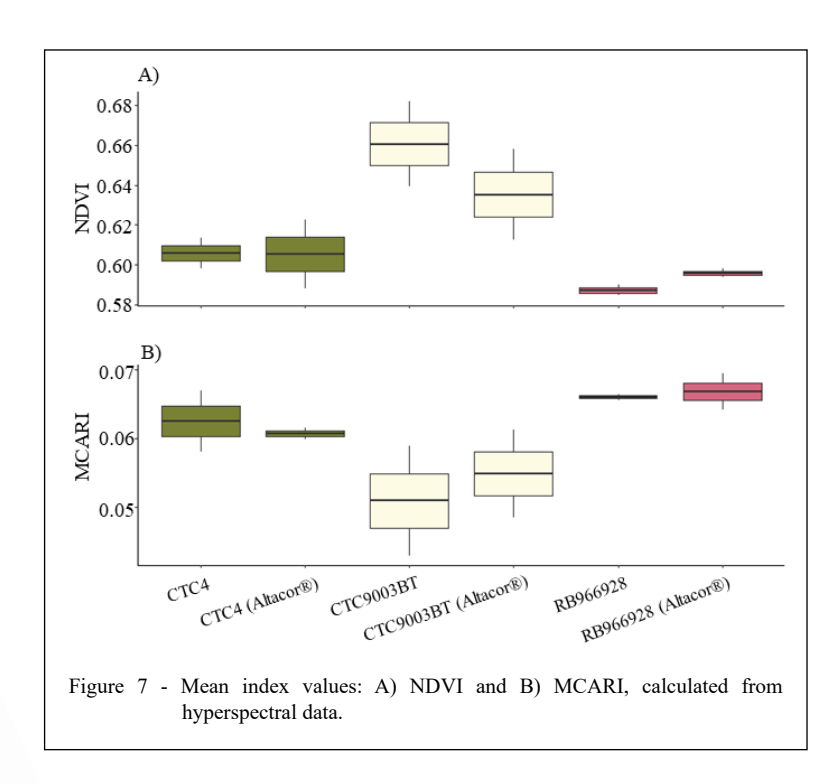


the red-edge region, allowing the different damage levels to be discriminated.

Red-edge normalized difference vegetation index (NDVI) and modified chlorophyll absorption ratio index (MCARI)

The representation of NDVI data using a box plot enabled better visualization and interpretation of the dataset (Figure 7). NDVI can vary due to several factors, making it difficult to associate it with a single

problem. Therefore, in this study, the varieties CTC, CTC9003BT, and RB966928 were placed in the same experimental environment, being exposed to the same contamination conditions by *D. saccharalis* and the insecticideAltacor, according to the treatment. In this sense, the variety with the highest mean NDVI was CTC9003BT, with a mean of 0.66, a minimum value of 0.63, and a maximum value of 0.75. The first quartile of collected information is 0.63 and the third quartile is 0.69.



Ciência Rural, v.55, n.3, 2025.

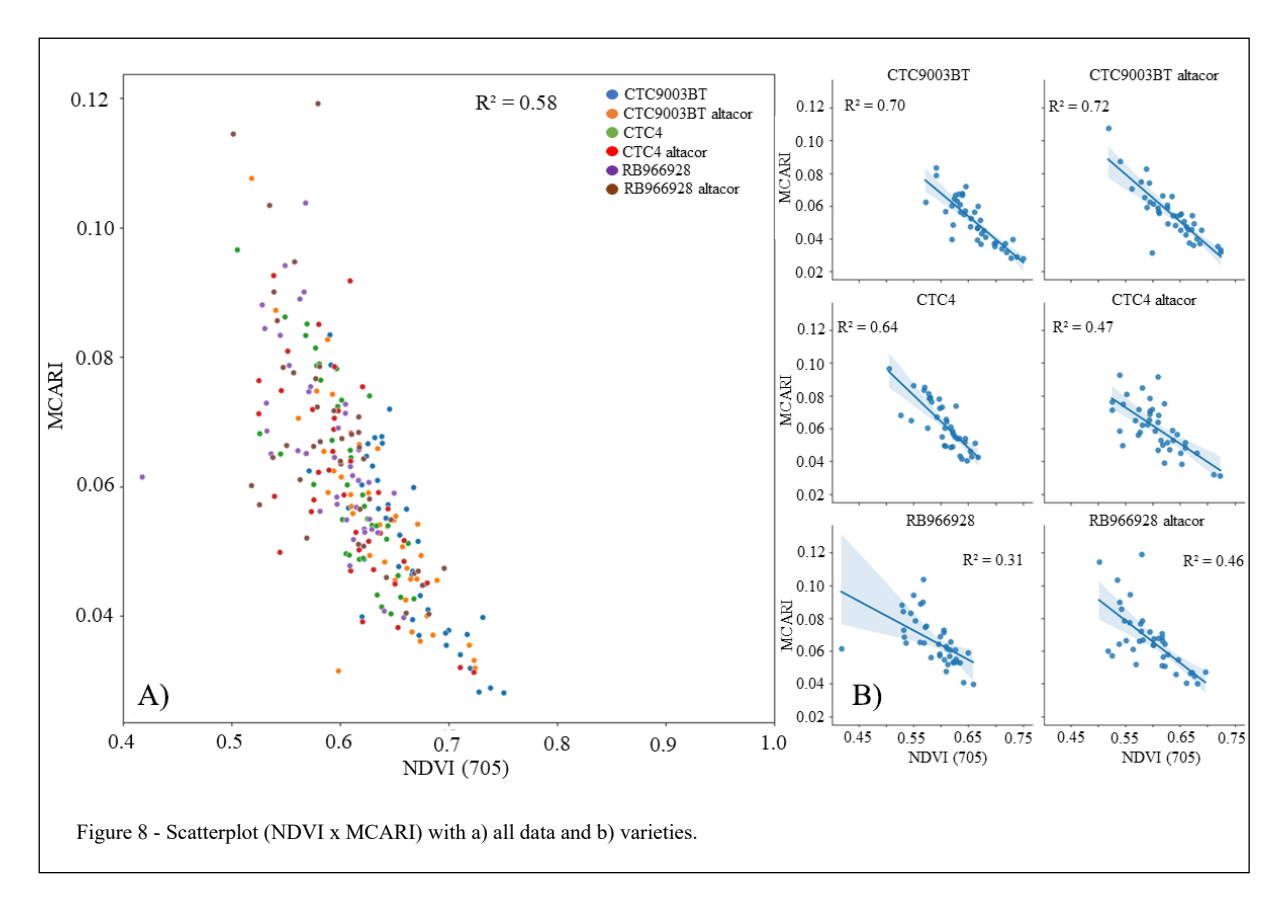
The variety CTC9003BT with insecticide Altacor was the second-best variety according to NDVI, with a mean and median of 0.64, first quartile of 0.60, third quartile of 0.67, and maximum of 0.72. The varieties CTC4 and CTC4 (with Altacor) presented the same behavior regarding the index, with a mean and median of 0.61, first quartile of 0.58, and third quartile of 0.63. The varieties RB966928 and RB966928 with Altacor also performed close to the median (0.60), but the mean for the former was lower, 0.59 compared to 0.60. However, the minimum information for the variety RB966928 was 0.42, while for the variety RB966928 Altacor was 0.50, with a maximum of 0.70 compared to 0.66 for the former.

KUNDU et al. (2021) monitored the severity of potato late blight disease using hyperspectral data and observed a decrease in NDVI from 0.61 in healthy plants to 0.3 as disease severity reached its highest level. Thus, the use of NDVI detected subtle variations in bio-optical responses caused by the diseased canopy.

Regarding MCARI, figure 7B shows the hyperspectral indices calculated for the varieties

with and without the application of the insecticide Altacor. The variety CTC9003BT had the lowest MCARI index. According to WU et al. (2008), lower values of this index are attributed to the high concentration of leaf chlorophyll. Consequently, the NDVI values were the highest for the same variety, meaning healthier plants. MARTINS & GALO (2015) observed lower MCARI values in healthy sugarcane compared to those infested with *M. fryanus* and nematodes, whereas lower NDVI values were found in the vegetation parasitized by the larva of the *M. fryanus*. Therefore, MARTINS & GALO (2015) suggested working on the indices together (NDVI and MCARI).

Scatterplots (NDVI x MCARI) were created to facilitate data visualization. Figure 8A ($R^2 = 0.58$) shows that the higher the NDVI, the lower the MCARI value. Figure 8B shows the analysis by variety separately and in detail. The plots containing CTC9003BT presented an $R^2 = 0.70$, while the plots with CTC9003BT Altacor generated an $R^2 = 0.72$. Plots with CTC4 had an R^2 of 0.64, while CTC4 Altacor showed an $R^2 = 0.47$. Finally, RB966928 generated an $R^2 = 0.31$ and RB966928 Altacor an $R^2 = 0.31$



Ciência Rural, v.55, n.3, 2025.

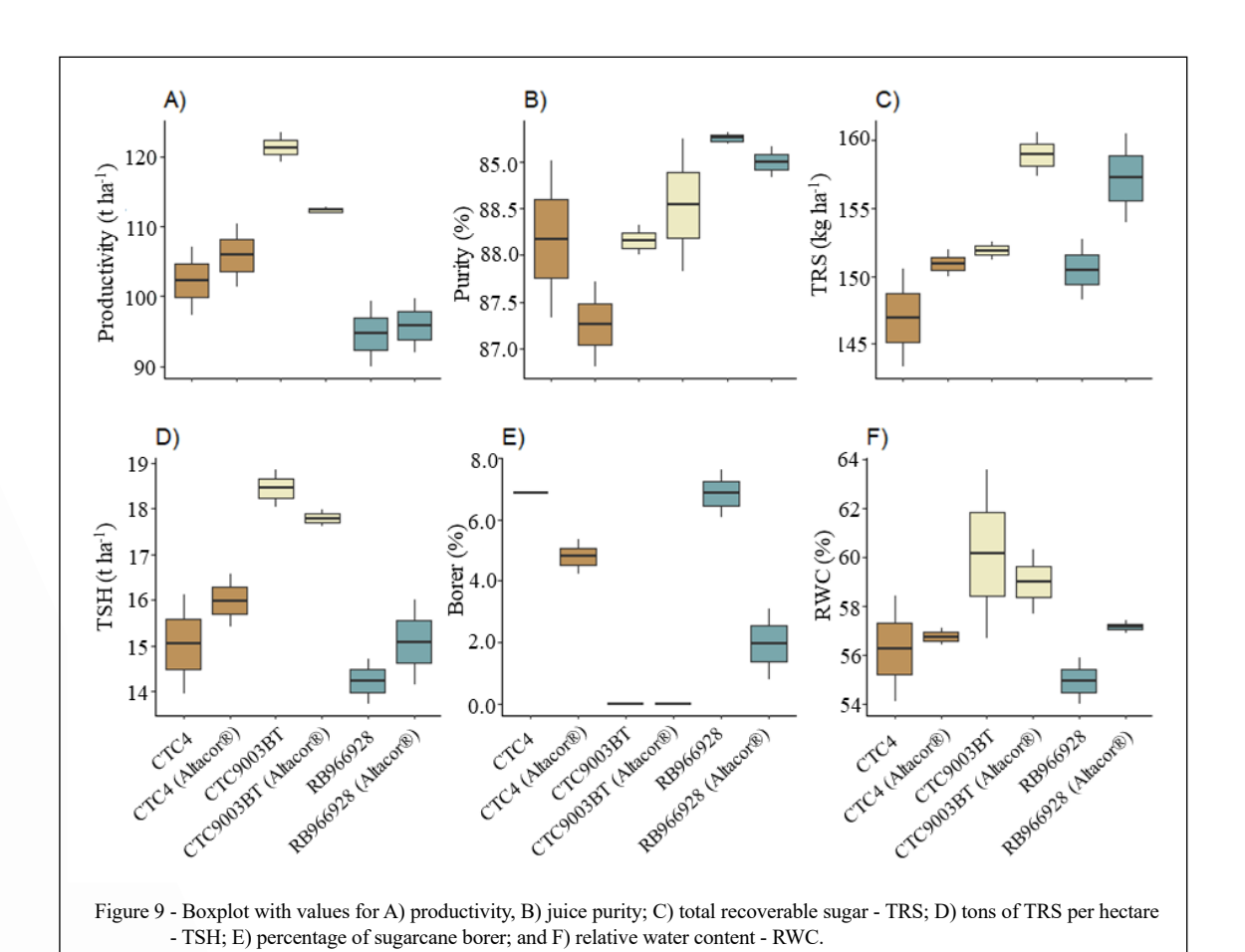
0.46. Therefore, the use of both indices was important to better understand the obtained values, as the variety CTC9003BT (with or without Altacor) presented satisfactory results, while the variety RB966928 (with or without Altacor) resulted in a lower correlation coefficient. In general, the information obtained using the two indices allowed us to predict, even if insignificantly, which plots would provide better or worse results in terms of productivity or intensity of infestation, for example.

Response of production, technology, water content (RWC), and infestation intensity parameters

The variety CTC9003BT without insecticide application presented the highest productivity (121.4 t ha⁻¹), followed by CTC9003BT (112.40 t ha⁻¹), CTC4 with Altacor (105.95 t ha⁻¹), and CTC4 without insecticide (102.26 t ha⁻¹). Except for CTC9003BT, the other varieties (CTC4 and RB966928) showed higher productivity when the insecticide was applied

(Figure 9A). Following the same productivity pattern, the TRS, TSH, and RWC values were higher for the variety CTC9003BT, in addition to presenting the lowest percentage of borer (0.0%). The water status of the studied varieties was assessed through water content (RWC), and the variety CTC9003BT without insecticide application had the highest percentage of RWC (60.15%), while RB966928 without insecticide application had the lowest value (54%) (Figure 9F). In contrast, RB966928 without insecticide application recorded the lowest RWC (54.9%) and productivity (94.6 t ha⁻¹) but the highest percentage of sugarcane borer (6.86%) (Figure 9E).

According to ROSSATO et al. (2013), high infestation levels (19.01 and 25.77%) negatively impact the raw material quality, as the borer increases sugarcane fiber and the contents of phenolic compounds in the extracted juice. In this sense, GALO et al. (2002) reported that borer control should begin as soon as final infestation intensity rates are above 3%.



Ciência Rural, v.55, n.3, 2025.

Pearson's correlation (r)

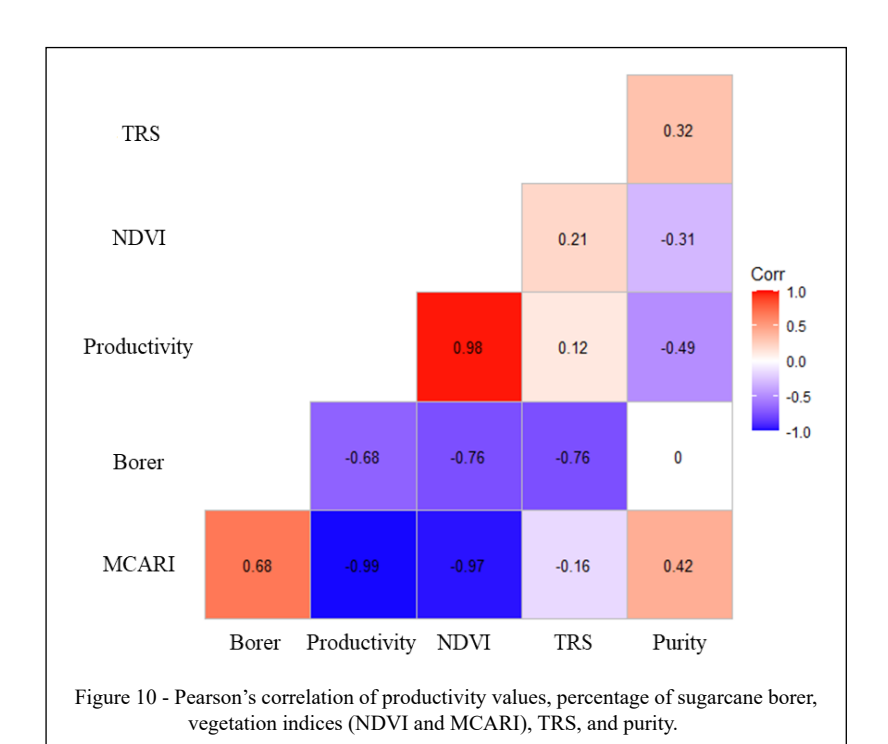
Figure 10 shows Pearson's correlation between productivity parameters, percentage of sugarcane borer, vegetation indices (NDVI and MCARI), TRS, and purity. The highest correlation coefficients were observed between productivity and NDVI and MCARI, with values of 0.98 and -0.99, respectively. NDVI had a positive linear correlation, indicating that increases in NDVI values are associated with increased productivity. This strong correlation between NDVI and sugarcane productivity has already been identified in other studies (AKBARIAN et al., 2022; BÉGUÉ et al., 2010; KAVATS et al., 2020; PINHEIRO LISBOA et al., 2018). Sugarcane is a dense cover crop with high reflectance in the nearinfrared spectrum, the band used to calculate NDVI, and hence these characteristics are related to the plant health and the ability to carry out photosynthesis, factors that contribute to the final crop productivity. However, the correlation between MCARI and productivity was high, but negative, suggesting that an increase in one variable is associated with a decrease in the other. This is consistent with the values of the MCARI index, as lower values of this index are attributed to a high concentration of leaf chlorophyll (WU et al., 2008). In other words, as MCARI values decrease, the chlorophyll concentration increases and, consequently, productivity increases, considering that the other factors limiting productivity are in balance.

The percentage of sugarcane borer also showed high and negative correlations between productivity, NDVI, and TRS, with coefficients of -0.68, -0.76, and -0.76, respectively. Although the coefficients are acceptable, they were all negative, suggesting that an increase in one variable is associated with a decrease in the other. Therefore, an increase in the percentage of sugarcane borer leads to a reduction in productivity, NDVI, and TRS. This fact was already expected, as the attack by the sugarcane borer leads to a reduction in stalk weight, a decrease in the sucrose content, breakage of the stalk by the wind, and aerial rooting (CARBOGNIN, 2019).

CONCLUSION

The principal component analysis (PCA) for the fourth collection - canopy (April 28, 2022) performed best relative to the others, corresponding to 98% of the spectral variability. The data uniformity of this collection allowed for choosing the vegetation indices that were used throughout the study, in addition to highlighting the influence and importance of the red-edge region.

The descriptive analysis of the spectral curves showed that the first collection (December 3, 2021) was not significant, as the leaves were



Ciência Rural, v.55, n.3, 2025.

young, and the central vein made readings difficult. Therefore, the choice of sugarcane development stages is essential for the precision of readings. The indices extracted from the canopy hyperspectral data (NDVI and MCARI) allowed the separation of more and less vigorous plots and varieties.

The influence of the red-edge region was mainly due to the feasibility of detecting structural or physiological changes in plants. Moreover, there was difficulty in diagnosing the occurrence of *D. saccharalis* or other pests in advance. The indices (NDVI and MCARI) also demonstrated sensitivity in identifying when the crop was undergoing some stress, but they can vary due to several factors, making it difficult to associate them with a single problem.

ACKNOWLEDGMENTS

To the Fundação de Estudos Agrários Luiz de Queiroz - FEALQ, for funding the publication of this research. To the Fundação de Amparo à Pesquisa do Estado de São Paulo (FAPESP), for funding the project no. 2013/22435-9, to which this research belongs, and to the Research and Projects Financing (FINEP), which allowed the acquisition of the spectroradiometer used in this research through the project PROSENSAP. And was financed in part by the Coordenação de Aperfeiçoamento de Pessoal de Nível Superior (CAPES), Brasil - Finance code 001.

DECLARATION OF CONFLICT OF INTEREST

The authors declare no conflict of interest. The funding sponsors had no role in the design of the study; in the collection, analyses, or interpretation of data; in the writing of the manuscript; and in the decision to publish the results.

AUTHORS' CONTRIBUTION

All authors contributed equally to the conception and writing of the manuscript. All authors critically revised the manuscript and approved the final version.

REFERENCES

ABDEL-RAHMAN, E. M. et al. Potential of spectroscopic data sets for sugarcane thrips (Fulmekiola serrata Kobus) damage detection. **International Journal of Remote Sensing**, v.31, n.15, p.4199-4216, 2010. Available from: https://doi.org/10.1080/01431160903241981. Accessed: Feb. 27, 2024. doi: 10.1080/01431160903241981.

AKBARIAN, S. et al. Sugarcane yields prediction at the row level using a novel cross-validation approach to multi-year multispectral images. **Computers and Electronics in Agriculture**, v.198, p.107024, 2022. Available from: https://doi.org/10.1016/j.compag.2022.107024. Accessed: Feb. 24, 2024. doi: 10.1016/j.compag.2022.107024.

ALVARES, C. A. et al. Köppen's climate classification map for Brazil. **Meteorologische Zeitschrift**, v.22, n.6, p.711-728, 2013.

Available from: https://doi.org/10.1127/0941-2948/2013/0507>. Accessed: Feb. 24, 2024. doi: 10.1127/0941-2948/2013/0507.

ASSUMPÇÃO, D. S. et al. Fluoreto emitido pelas indústrias cerâmicas reduz a produtividade do milho em Cesário Lange-SP. **Brazilian Journal of Development**, v.6, n.5, p.28703-28713, 2020. Available from: https://doi.org/10.34117/bjdv6n5-351. Accessed: Feb. 20, 2024. doi: 10.34117/bjdv6n5-351.

BARROS, P. P. S. et al. Monitoring Bemisia tabaci (Gennadius) (Hemiptera: Aleyrodidae) Infestation in Soybean by Proximal Sensing. **Insects**, v.12, n.1, p.47, 2021. Available from: https://doi.org/10.3390/insects12010047>. Accessed: Feb. 20, 2024. doi: 10.3390/insects12010047.

BAUER, M. E. Spectral inputs to crop identification and condition assessment. **Proceedings of the IEEE**, v.73, n.6, p.1071-1085, 1985. Available from: https://doi.org/10.1109/PROC.1985.13238. Accessed: Feb. 10, 2024. doi: 10.1109/PROC.1985.13238.

BÉGUÉ, A. et al. Spatio-temporal variability of sugarcane fields and recommendations for yield forecast using NDVI. **International Journal of Remote Sensing**, v.31, n.20, p.5391–5407, 2010. Available from: https://doi.org/10.1080/01431160903349057. Accessed: Feb. 10, 2024. doi: 10.1080/01431160903349057.

CANABARRO, N. I. et al. Sustainability assessment of ethanol and biodiesel production in Argentina, Brazil, Colombia, and Guatemala. **Renewable and Sustainable Energy Reviews**, v.171, p.113019, 2023. Available from: https://doi.org/10.1016/j.rser.2022.113019. Accessed: Feb. 10, 2024. doi: 10.1016/j.rser.2022.113019.

CARBOGNIN, É. R. Modelagem de previsão de Diatraea saccharalis (Fabricius, 1794) (*Lepidoptera: Crambidae*) em cana-de-açúcar (*Saccharum* spp.). Jabotical: Universidade Estadual Paulista, 2019. Available from: http://hdl.handle.net/11449/191507>. Accessed: Feb. 09, 2024.

CARBOGNIN, É. R. et al. Unraveling the effect of temperature and humidity on the life cycle of Diatraea saccharalis (*Lepidoptera*: *Crambidae*) and the impact on pest outbreaks. **Environmental Entomology**, v.52, n.6, p.1139-1151, 2023. Available from: https://doi.org/10.1093/ee/nvad095>. Accessed: Feb. 10, 2024. doi: 10.1016/j.rser.2022.113019.

CARTER, G. A. Primary and secondary effects of water content on the spectral reflectance of leaves. **American Journal of Botany**, v.78, n.7, p.916-924, 1991. Available from: https://doi.org/10.1002/j.1537-2197.1991.tb14495.x. Accessed: Feb. 10, 2024. doi: 10.1002/j.1537-2197.1991.tb14495.x.

CHEN, T. et al. Detection of Stress in Cotton (*Gossypium hirsutum* L.) Caused by Aphids Using Leaf Level Hyperspectral Measurements. **Sensors**, v.18, n.9, p.2798, 2018. Available from: https://doi.org/10.3390/s18092798>. Accessed: Feb. 10, 2024. doi: 10.3390/s18092798.

CHO, M. A.; SKIDMORE, A. K. A new technique for extracting the red edge position from hyperspectral data: The linear extrapolation method. **Remote Sensing of Environment**, v.101, n.2, p.181-193, 2006. Available from: https://doi.org/10.1016/j.rse.2005.12.011. Accessed: Feb. 10, 2024. doi: 10.1016/j.rse.2005.12.011.

CLEVERS, J. G. P. W. et al. Derivation of the red edge index using the MERIS standard band setting. **International Journal of Remote Sensing**, v.23, n.16, p.3169-3184, 2002. Available from:

- https://doi.org/10.1080/01431160110104647. Accessed: Feb. 10, 2024. doi: 10.1080/01431160110104647.
- CTC Centro de Tecnologia Canavieira. **Bula Técnica CTC20BT**. Centro de Tecnologia Canavieira, 20p, 2017. Available from: http://www.ctc.com.br/>. Accessed: Feb. 10, 2024.
- CTC Centro de Tecnologia Canavieira. **Bula Técnica CTC9003BT (Alta performance e eficácia no combate a broca)**. Centro de Tecnologia Canavieira, 9p, 2021. Available from: http://www.ctc.com.br/>. Accessed: Feb. 10, 2024.
- CUNDILL, S.; et al. Adjusting spectral index for Spectral Response Function Differences of Very High Spatial Resolution Sensors Simulated from Field Spectra. **Sensors**, v.15, n.3, p.6221-6240, 13 mar. 2015. Available from: https://doi.org/10.3390/s150306221. Accessed: Feb. 10, 2024. doi: 10.3390/s150306221.
- DAUGHTRY, C. Estimating cornl Leaf Chlorophyll Concentration from Leaf and Canopy Reflectance. **Remote Sensing of Environment**, v.74, n.2, p.229-239, 2000. Available from: https://doi.org/10.1016/S0034-4257(00)00113-9. Accessed: Feb. 10, 2024. doi: 10.1016/S0034-4257(00)00113-9.
- FIORIO, P. R. et al. Prediction of leaf nitrogen in sugarcane (Saccharum spp.) by vis-NIR-SWIR spectroradiometry. **Heliyon**, p.e26819, 2024. Available from: https://doi.org/10.1016/j.heliyon.2024.e26819. Accessed: Feb. 10, 2024. doi: 10.1016/j.heliyon.2024.e26819.
- FOGLIATA, S. V. et al. Unraveling the population structure of the sugarcane borer, *Diatraea saccharalis*, in Argentina. **Entomologia Experimentalis et Applicata**, v.170, n.6, p.530-545, 2022. Available from: https://doi.org/10.1111/eea.13174>. Accessed: Feb. 10, 2024. doi: 10.1111/eea.13174.
- FRANCESCHINI, M. H. D. et al. Semi-quantitative and quantitative approaches in soil texture assessment by bidirectional reflectance spectroscopy in the VIS-NIR-SWIR. **Pesquisa Agropecuária Brasileira**, v.48, n.12, p.1569-1582, 2013. Available from: https://doi.org/10.1590/S0100-204X2013001200006. Accessed: Feb. 10, 2024. doi: 10.1590/S0100-204X2013001200006.
- GALLO, D. et al. **Entomologia agrícola**. Piracicaba: Biblioteca de Ciências Agrárias Luiz de Queiroz, 2002. v.10.
- HATFIELD, J. L. et al. Application of spectral Remote Sensing for Agronomic Decisions. **Agronomy Journal**, v.100, n.S3, 2008. Available from: https://doi.org/10.2134/agronj2006.0370c. Accessed: Feb. 10, 2024. doi: 10.2134/agronj2006.0370c.
- JONG, S. M. et al. The spectral response of Buxus sempervirens to different types of environmental stress A laboratory experiment. **ISPRS Journal of Photogrammetry and Remote Sensing**, v.74, p.56-65, 2012. Available from: https://doi.org/10.1016/j.isprsjprs.2012.08.005. Accessed: Feb. 10, 2024. doi: 10.1016/j. isprsjprs.2012.08.005.
- KAVATS, O. et al. Monitoring of sugarcane Harvest in Brazil Based on Optical and SAR Data. **Remote Sensing**, v.12, n.24, p.4080, 2020. Available from: https://doi.org/10.3390/rs12244080>. Accessed: Feb. 10, 2024. doi: 10.3390/rs12244080.
- KUNDU, R. et al. Near real Time Monitoring of Potato Late Blight Disease Severity using Field Based Hyperspectral Observation. **Smart Agricultural Technology**, v.1, p.100019, 2021. Available

- from: https://doi.org/10.1016/j.atech.2021.100019>. Accessed: Feb. 10, 2024. doi: 10.1016/j.atech.2021.100019.
- LASSALLE, G. Monitoring natural and anthropogenic plant stressors by hyperspectral remote sensing: Recommendations and guidelines based on a meta-review. **Science of The Total Environment**, v.788, p.147758, 2021. Available from: https://doi.org/10.1016/j.scitotenv.2021.147758. Accessed: Feb. 10, 2024. doi: 10.1016/j.scitotenv.2021.147758.
- LIU, X.-D.; SUN, Q.-H. Early assessment of the yield loss in rice due to the brown planthopper using a hyperspectral remote sensing method. **International Journal of Pest Management**, v.62, n.3, p.205-213, 2016. Available from: https://doi.org/10.1080/09670874.2016.1174791>. Accessed: Feb. 10, 2024. doi: 10.1080/09670874.2016.1174791.
- MARTINS, G. D.; GALO, M. DE L. B. T. Caracterização espectral da cana-de-açúcar infectada por nematoides e migdolus fryanus por espectrorradiometria de campo. **Boletim de Ciências Geodésicas**, v.21, n.4, p.783-796, 2015. Available from: https://doi.org/10.1590/S1982-21702015000400046. Accessed: Feb. 10, 2024. doi: 10.1590/S1982-21702015000400046.
- MORAES NOVO, E. M. L. Sensoriamento Remoto: princípios e aplicações.1 ed. Editora Blucher, 2010. 388 p.
- MULLA, D. J. Twenty-five years of remote sensing in precision agriculture: Key advances and remaining knowledge gaps. **Biosystems Engineering**, v.114, n.4, p.358-371, 2013. Available from: https://doi.org/10.1016/j.biosystemseng.2012.08.009. Accessed: Feb. 10, 2024. doi: 10.1016/j.biosystemseng.2012.08.009.
- OLIVEIRA, W. S. et al. Varied frequencies of resistance alleles to Cry1Ab and Cry1Ac among Brazilian populations of the sugarcane borer, Diatraea saccharalis (F.). **Pest Management Science**, v.78, n.12, p.5150-5163, 2022. Available from: https://doi.org/10.1002/ps.7133. Accessed: Feb. 10, 2024. doi: 10.1002/ps.7133.
- PINHEIRO LISBOA, I. et al. Prediction of Sugarcane Yield Based on NDVI and Concentration of Leaf-Tissue Nutrients in Fields Managed with Straw Removal. **Agronomy**, v.8, n.9, p.196, 2018. Available from: https://doi.org/10.3390/agronomy8090196>. Accessed: Feb. 10, 2024. doi: 10.3390/agronomy8090196.
- PINTER, J. R., P. J. et al. Remote Sensing for Crop Management. **Photogrammetric Engineering & Remote Sensing**, v.69, n.6, p.647-664, 2003. Available from: https://doi.org/10.14358/PERS.69.6.647. Accessed: Feb. 10, 2024. doi: 10.14358/PERS.69.6.647.
- PRASANNAKUMAR, N. R.; et al. Characterization of brown planthopper damage on rice crops through hyperspectral remote sensing under field conditions. **Phytoparasitica**, v.42, n.3, p.387-395, 2014. Available from: https://doi.org/10.1007/s12600-013-0375-0. Accessed: Jan. 10, 2024. doi: 10.1007/s12600-013-0375-0.
- RIBEIRO, L. A. L. **Use of hyperspectral data for the differentiation of sugarcane (Saccharum officinarum) L varieties**. [Tese de Doutorado]. Piracicaba: Universidade de São Paulo, 2022. Available from: https://doi.org/10.11606/D.11.2022.tde-11082022-095930. Accessed: Feb. 10, 2024.
- RIDESA Rede Interuniversitária para o Desenvolvimento do Setor Sucroalcooleiro. Catálogo nacional de variedades "RB" de cana-de-açúcar. Curitiba: Ridesa Brasil; 2010. Available from:

http://www.cana.com.br/biblioteca/informativo/catalogo-2010.pdf>. Accessed: Feb. 24, 2024.

ROSSATO, J. A. et al. Characterization and impact of the Sugarcane Borer on Sugarcane Yield and Quality. **Agronomy Journal**, v.105, n.3, p.643-648, 2013. Available from: https://doi.org/10.2134/agronj2012.0309>. Accessed: Feb. 10, 2024. doi: 10.2134/agronj2012.0309.

SILALERTRUKSA, T.; GHEEWALA, S. H. Competitive use of sugarcane for food, fuel, and biochemical through the environmental and economic factors. **The International Journal of Life Cycle Assessment**, v.25, n.7, p.1343-1355, 2020. Available from: https://doi.org/10.1007/s11367-019-01664-0. Accessed: Feb. 20, 2024. doi: 10.1007/s11367-019-01664-0.

SILVA et al. Detection of nutritional stress in sugarcane by VIS-NIR-SWIR reflectance spectroscopy. **Ciência Rural**, v.53, n.12, 2023. Available from: https://doi.org/10.1590/0103-8478cr20220543. Accessed: Feb. 10, 2024. doi: 10.1590/0103-8478cr20220543.

SILVA JUNIOR, J. A.; PACHECO, A. D. P. Avaliação de incêndio em ambiente de Caatinga a partir de imagens Landsat-8, índice de vegetação realçado e análise por componentes principais. **Ciência Florestal**, v.31, n.1, p.417-439, 2021. Available from: https://doi.org/10.5902/1980509843818. Accessed: Feb. 10, 2024. doi: 10.5902/1980509843818.

MEDINA, G.; POKORNY, B. Agro-industrial development: Lessons from Brazil. Land Use Policy, v.120, p.106266, 2022. Available from: https://doi.org/10.1016/j.landusepol.2022.106266. Accessed: Feb. 10, 2024. doi: 10.1016/j.landusepol.2022.106266.

SINCLAIR, T. R.; et al. Reflectance and Internal Structure of Leaves from Several Crops During a Growing Season. **Agronomy Journal**, v.63, n.6, p.864-868, 1971. Available from: https://doi.org/10.2134/agronj1971.00021962006300060012x. Accessed: Feb. 10, 2024. doi: 10.2134/agronj1971.00021962006300060012x.

STRABELI, T. F. et al. Conteúdo relativo de água afeta o comportamento espectral de folhas de Eucalyptus spp. Scientia

Forestalis, v.48, n.128, 2020. Available from: https://doi.org/10.18671/scifor.v48n128.25>. Accessed: Feb. 10, 2024. doi: 10.18671/scifor.v48n128.25.

STRABELI, T. F. et al. Modelos espectrais para a estimativa do conteúdo de água em folhas de Eucalyptus. **Scientia Forestalis**, v.51, 2023. Available from: https://doi.org/10.18671/scifor.v50.49. Accessed: Jan. 10, 2024. doi: 10.18671/scifor.v50.49.

TAVARES, T. R. Espectroscopia de reflectância in situ na avaliação da resposta da adubação nitrogenada em cana-de-açúcar. Piracicaba: Universidade de São Paulo, 2017. Available from: https://doi.org/10.11606/D.11.2017.tde-09082017-164610. Accessed: Feb. 10, 2024. doi: 10.11606/D.11.2017.tde-09082017-164610.

TURDERA, M. V. Energy balance, forecasting of bioelectricity generation and greenhouse gas emission balance in the ethanol production at sugarcane mills in the state of Mato Grosso do Sul. **Renewable and Sustainable Energy Reviews**, v.19, p.582-588, 2013. Available from: https://doi.org/10.1016/j.rser.2012.11.055. Accessed: Jan. 21, 2024. doi: 10.1016/j.rser.2012.11.055.

WU, C. et al. Estimating chlorophyll content from hyperspectral vegetation indices: Modeling and validation. **Agricultural and Forest Meteorology**, v.148, n.8-9, p.1230–1241, 2008. Available from: https://doi.org/10.1016/j.agrformet.2008.03.005. Accessed: Jan. 20, 2024. doi: 10.1016/j.agrformet.2008.03.005.

ZHANG, J. et al. Advances in estimation methods of vegetation water content based on optical remote sensing techniques. **Science China Technological Sciences**, v.53, n.5, p.1159-1167, 2010. Available from: https://doi.org/10.1007/s11431-010-0131-3. Accessed: Feb. 10, 2024. doi: 10.1007/s11431-010-0131-3.

ZHAO, X. et al. Evaluating the potential of airborne hyperspectral LiDAR for assessing forest insects and diseases with 3D Radiative Transfer Modeling. **Remote Sensing of Environment**, v.297, p.113759, 2023. Available from: https://doi.org/10.1016/j.rse.2023.113759. Accessed: Feb. 10, 2024. doi: 10.1016/j. rse.2023.113759.